IJBEM
Vol. 7, No. 2, 2005

Fast Localization of Current Dipoles in MEG Using a Combined Sphere and Brain-Shape Model

Hongyi Zhu[1], Gunnar Lindenblatt[1] and Sailing He[1,2]
[1]Centre for Optical and Electromagnetic Research, State Key Laboratory of Modern Optical Instrumentation, Zhejiang University, Hangzhou 310027, China.
[2] Division of Electromagnetic Theory, Alfven Laboratory, Royal Institute of Technology, S-100 44 Stockholm, Sweden

Abstract—**By combining the advantages of the simple sphere model (fast computing speed) and the realistic brain-shape model (high accuracy), a combined model for magnetoencephalography (MEG) is introduced to localize a current dipole inside a human brain. A geometrical description of the difference between the sphere model and the brain-shape model is obtained and used to divide the brain into ``large difference areas (LDAs)'' and ``small difference areas (SDAs)''. The current dipole is localized with an optimization method, in which the sphere and brain-shape models are used when the trial dipole is located in an SDA and an LDA, respectively. The present method is fast while keeping a reasonably good accuracy.**

Keywords—**MEG, sphere model, realistic model, combined model, BEM, current dipole, localization, genetic algorithm**

I. Introduction

Magnetoencephalography (MEG) [1] is a method for determining brain activities by measuring the magnetic field non-invasively outside a human head. Since the neuromagnetic field is very weak (50—500 fT), it is usually measured by superconducting quantum interference devices (SQUIDs). In many cases, the neuromagnetic sources can be modeled by several current dipoles that are appropriate for interpreting postsynaptic potentials occurred in active neurons, and one wishes to localize these current dipoles. MEG has become a promising technique for brain functional study/imaging and diagnosis of brain diseases.

For decades, the simple sphere model has been widely used in MEG for calculating scalp potentials and external magnetic fields resulted from the current dipoles. However, further studies for more realistic models revealed that the sphere model is not accurate enough for computing the magnetic field of a dipole source located in some special areas of the brain[2-5]. Typically, three layers are used in realistic head model: the scalp, the skull and brain tissue (including the gray and white matters as well as the cerebrospinal fluid)[1]. The boundaries of these layers are used in a boundary element method (BEM) to solve the forward problem, i.e., to calculate the external magnetic field for a known dipole source. Although the BEM takes longer computation time and requires larger computer memory [4, 6] as compared with the sphere model, this model still plays an important role in MEG studies.

In the present paper, we introduce a combined model to keep the advantages of both the sphere model and the brain-shape model. The difference in the "measured" magnetic fields derived from the sphere model and a single-layered realistic head model([3], call "the brain-shape model" hereafter) is calculated for many test positions of the dipole. We thus obtain a geometrical description of the relative difference between these two models. According to this description, we then divide the brain into small difference areas (SDAs) where the relative difference is less than a threshold, and the large difference areas (LDAs) where the relative difference is larger than the threshold. The localization of the current dipole is solved with an optimization method, in which the sphere and brain-shape models are used when the trial dipole is located in an SDA and an LDA, respectively. Speed and accuracy of the present combined model are compared with those of the simple sphere model and the accurate brain-shape model.

II. Method

First we need to define each LDA. Several authors have investigated the difference between the sphere model and a more realistic head model and obtained similar conclusions [2, 4, 7]:

1. The scalp and skull have little influence on the accuracy of the localization.
2. Obvious differences between the sphere model and the brain-shape model exist only in a few small areas.
3. These small areas can be identified with anatomical structures of the brain, and the division of these small areas is almost the same for different patients.

Unfortunately, the authors of these papers just gave some rough expression such as ``deep source", ``near the bottom of the skull in frontotemporal and frontal areas"[2], but not an accurate expression for the areas where the sphere model does not work well. In our method, we must know whether a trial dipole is located in an LDA or SDA. This requires a precise division of the brain. Since such a division is insensitive to individual anatomy (of different patients), the division can be transferred from one patient to other patients.

For each position of the trial dipole, we obtain the difference between the external magnetic fields calculated by the sphere model[8] and the brain-shape model[3] at various measurement points. Point by point, we can obtain a geometrical description of the difference between the sphere model and the brain-shape model. According to this description, we can define an LDA as a part where the difference is relatively large (larger than a threshold value). The brain surface is discretised with 1296 vertices and 2588 triangles (see Fig. 1.), and the mass center of the brain is chosen as the center of the sphere in the sphere model. Then the straight lines between the center of the sphere and the surface vertices form 1296 radii. The trial dipole is placed at 120 different positions on each radius (40 positions close to the center with an interval of r/80, and 80 positions close to the node with an interval of r/160, where r is the radius). Thus, a total of 155520 dipole positions in a brain are chosen and the corresponding magnetic fields are

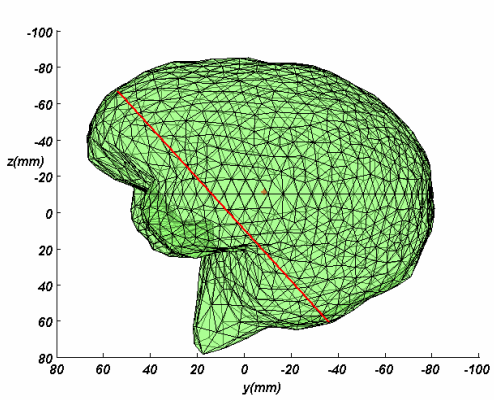

Fig. 1. Triangularization of the brain considered in the present paper.

calculated using both the sphere model and the brain-shape model. Here the trial dipole is oriented along a tangential direction at each position. The relative difference between the external magnetic fields calculated with the sphere (SP) model and the brain-shape (BS) model is defined by:

$$B^* = \frac{\sum_{i=1}^{n}(B_{SP} - B_{BS})^2}{\sum_{i=1}^{n} B_{BS}^{\ 2}}$$

where n is the total number of the measurement points. The relative difference B* for each dipole position is shown in Fig. 2 and the points where $B^* \geq 0.5$ are shown in Fig. 3. The ratio of the points in each specific range of B^* is shown in Fig. 4.

From Figs 2-4 one sees that B* is less than 0.2 at many points (about 36.3% of all the testing points), which means that in the areas formed by these points the sphere model gives almost the same result as the brain-shape model. However, there exist many dipole positions where the relative difference B* is large: 6.4% with $0.5 \leq B^* \leq 1$, and 10.1% with $B^* \geq 1$.

Fortunately, the positions where the sphere model and the brain-shape model result in large differences are concentrated in five areas (see Figs 2 and 3): the first one is an area around the brain mass center. The second, third and fourth areas can be found near the surface of the lower part

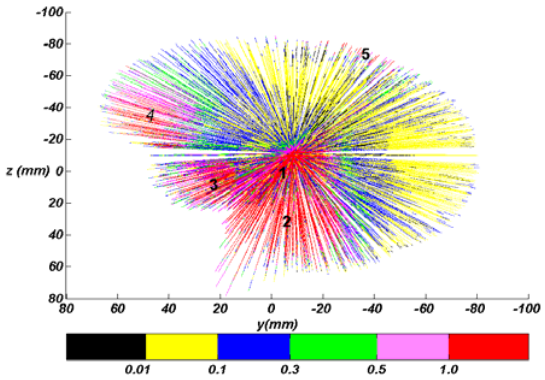

Fig. 2. The distribution of the relative difference B* between the magnetic fields calculated with the brain-shape model and the sphere model when the trial dipole is located at 155520 different positions. These values are divided into 6 intervals and displayed with 6 different colors (see the color bar). The five LDAs (with difference B^* larger than 0.5) are marked with numbers 1, 2...5 in this figure.

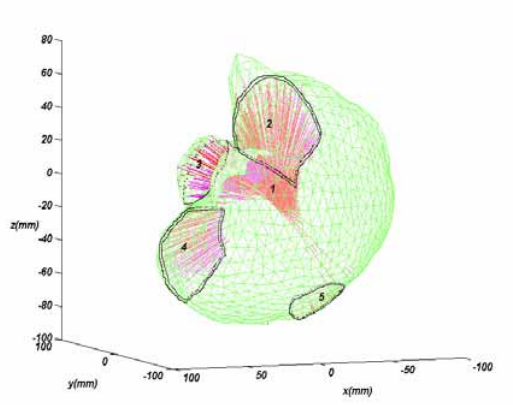

Fig. 3. A 3D view of the meshed surface of the brain with the five LDAs marked.

of the brain where its shape is irregular (quite different from a sphere). These areas consist of the cerebellum, the temporal lobe, and the deep prefrontal area. The fifth one is a very small area located at the upper smooth ``sphere like'' part (the parietal lobe) of the brain. In addition, the difference B^* varies continuously in the brain: in the color-coded representation of Fig. 2, we found B* varies smoothly through all colors. We can choose a certain threshold B^*_{th} for relative difference B^* to define the LDA. Here we choose $B^*_{th} = 0.5$.

For convenience, we approximate each LDA to some simple geometrical structure (such a combined model is referred to the local brain-shape model hereafter). Among these five LDAs, the first area is the largest one, which is shown separately in Fig. 5. From this figure one can see that this area has a shape similar to a lotus flower. We can approximate it with two connected cones of different obliquity (see Fig.5.)

The second area is a ``bent plate'', which is localized in the area surrounded by the three poping-out parts in the lower part of the brain. We replace it with a disk of 20mm thick. The boundary of its bottom surface is mainly formed by the natural boundary of the brain (see Fig. 3). The upper surface is parallel to this bottom surface and has the same shape.

The third area is the poping-out parts of the temporal lobe, and the forth area is the left front part of the frontal lobe (15mm thick; see Fig. 2). The fifth area can be approximated as a disk.

Since the relative difference B* varies continuously with the position of the trial dipole, the boundary of LDA is not so strict (a change of the threshold B^*_{th} will enlarge or reduce a bit the above-described areas).

We assign these five areas as LDAs and the rest of the brain as SDAs. In this way, our local brain-shape model is established.

Further simplification can also be made. Since the second, third and fourth LDAs are located at the lower part of the brain, these areas can be replaced by a single LDA formed the area under the red line in Fig. 1 (the full irregular lower part of the brain). In other words, we use a plane to divide the brain into two parts: the lower part belongs to the LDA, and the upper part is the SDA except the first and fifth LDAs. This simplified model (called a

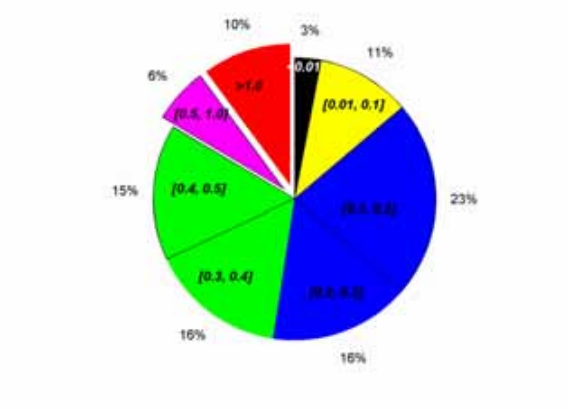

Fig. 4. The ratio of the number of the points in each range of relative difference B^*.

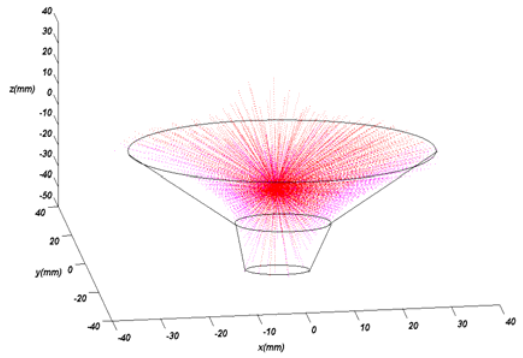

Fig. 5. Enlarged view of the first LDA (around the brain mass center) and the simple geometrical structure used to approximate this LDA.

half-sphere model hereafter) is much easier to construct. We use an optimization method to estimate the parameters of the dipole source. To avoid the problem of local minima, the genetic algorithm [a global optimization method; see e.g. [9]] is adopted in the present paper. During the search process, when a trial current dipole is located in a small difference area (SDA), we use the sphere model to calculate the forward solution. When the trial current dipole is located in a large difference area (LDA), we use the brain-shape model. The present method can also work for the case of multiple dipole sources.

III. Results and Discussion

Here we use a brain-shape model to calculate the magnetic fields of some pre-placed dipoles and add 5% Gaussian white noise as the input data for the localization. First we solve the localization of a single dipole for 155 520 situations to test the generality. The dipole positions are chosen in various areas as described in section 3. The results of localization are shown in Figs. 6 and 7. From these two figures one sees that both the half-sphere model and the local brain-shape model work well, and localization error larger than 5mm occurs only at a few dipole positions. Furthermore, in the LDA the half-sphere model gives a better localization at some points than the local brain-shape model. That's because some approximate geometrical body is used to replace the realistic LDA in the local brain-shape model and there exist a few points near the SDA boundary (in the lower area of the brain) where BEM should be used (but we use the sphere model in the local brain-shape model). Next we apply the genetic algorithm to localize two dipoles in the brain based on the brain-shape model, the sphere model, the half-sphere model and the local brain-shape model. Three cases are tested: (1) both dipoles are in LDA, (2) both dipoles are in SDA and (3) one dipole in LDA and another in SDA. We compare the accuracy and speed of the localization for these four models (for the case of the dipole pair so that we can also see the robustness of the present method for such a more complicated case). The true and reconstructed locations for these dipoles are given in Table I, and the corresponding computation times are given in Table II. The momentum of each dipole is assumed to be (1; 0; 0) (with an arbitrary unit). Regarding the accuracy, all models except the sphere model give similar results. The sphere model fails in the LDA, as expected. Concerning the speed, the brain-shape model is much slower than the other three models. Depending on the location of the dipole source in LDA or SDA, the brain-shape model is about 4.5 to 6 times slower than the other three models. The sphere model is the fastest and the local brain-shape model is the second fastest. For a dipole located in an LDA, the speed difference among these three models is smaller than that for a dipole located in an SDA. During

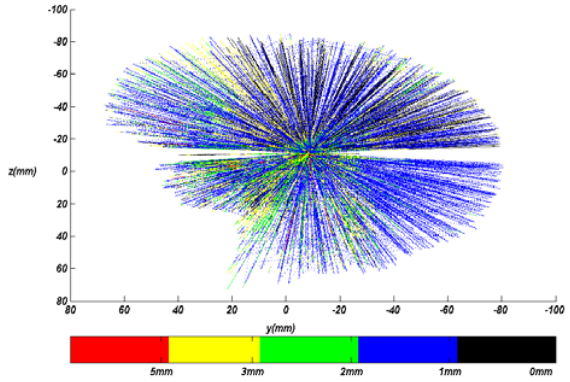

Fig. 6. The distribution of the localization error using the half-sphere model. 155520 dipoles are used one by one in the calculation, and the values of the localization error are divided into 5 ranges and displayed with different colors.

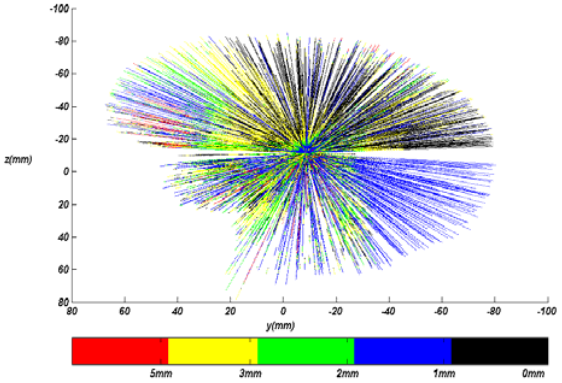

Fig. 7. The distribution of the localization error for the same situation of Figure 10 but using the local brain-shape model.

the search process, we will get closer to the true location step by step. If the true dipole location is inside an LDA, BEM have to be run more times and thus more computation time is needed. (the computation speed given in Table IV may look slower than those of other methods[10-12] since the pre-calculation times, which sometimes are several ten hours, are excluded in their work).

Table I. The errors of localization (with unit of mm; along z, y and z axes) using the (pure) brain-shape model (BSM), the (pure) sphere model (SM), the local brain-shape model (LBSM), and the half-sphere model (HSM).

True position (mm)	Localization errors for the dipoles (mm)			
	SM	BSM	LBSM	HSM
(-59;2;1)	(0.7;0.9;2.1)	(-0.4;0.5;1.6)	(0.6;0.5;1.8)	(0.2;0.3;1.3)
(-3;-80;-7)	(0.4;1.2;1.9)	(0.6;0.4;1.4)	(0.5;0.2;1.6)	(0.2;0.6;1.6)
(-59; 2; 1)	(1.2;0.2;2.4)	(0.8;0.3;0.3)	(0.9;0.2;0.4)	(0.7;0.5;1.2)
(10;-20;10)	(12.4;17.4;13.3)	(1.3;0.3;1.2)	(0.8;1.2;1.3)	(0.3;0.6;1.4)
(10;-20;10)	(25.2;-9.6;13.1)	(0.2;0.5;1.3)	(0.2;0.5;1.6)	(0.3;0.4;0.2)
(-2;-10;-12)	(20.5;14.4;32.3)	(0.2;0.3;2.3)	(0.3;0.2;1.5)	(-1.8;0.5;1.8)

The tolerant error for termination for the GMRES method is set to 10^{-6}.

Table II. The time spent in the genetic algorithm for the localization of dipoles with different brain models.

Dipole pair (mm)	Computing time (second)			
	SM	BM	LBSM	HSM
(-59; 2; 1)(-3; -80; -7)	69.5	430.6	73.1	92.3
(-59; 2; 1)(10; -20; 10)	68.8	431.2	78.9	103.9
(10;-20;10)(-2;-10;-12)	69.1	430.4	82.5	109.6

All the time data are obtained using a Matlab code running on a PC (Pentium IV, 2.8GHz, 2GB RAM). The time data listed here do not include any pre-calculation time.

IV. Conclusion

We have introduced a combined model, to localize efficiently a current dipole source in MEG. Through a comprehensive comparison, we divided the brain into large difference areas (LDAs) and small difference areas (SDAs). In an SDA, the sphere model has almost the same accuracy as the realistic head model, whereas in an LDA the sphere model and the realistic head model will give quite different results. We use the sphere model when the dipole is located in an SDA, and use the realistic head model when the dipole is located in an LDA. Our numerical results for various localization problems containing one or two dipoles have shown that the present localization algorithm is much faster (while keeping the same accuracy) than the direct BEM method for the brain-shape model.

Acknowledgment

This work is supported by the National Natural Science Foundation of China (under grant no.30000034 and no.60372032).

References

[1] M. S. Hämäläinen, R. Hari, R. J. Ilmoniemi, J. Knuutila, and O. V. Lounasmaa, "Magnetoencephalography: Theory, instrumentation, and applications to noninvasive studies of the working human brain," *Reviews of Modern Physics*, vol. 65, pp. 413-497, 1993.

[2] M. S. Hämäläinen, J. Sarvas, " Feasibility of the homogeneous head model in the interpretation of neuromagnetic fields," *Phys. Med. Biol.*, vol. 32, pp. 91-97, 1987.

[3] M. S. Hämäläinen, J. Sarvas, "Realistic conductivity geometry model of the human head for interpretation of neuromagnetic data," *IEEE Trans. Biomed. Eng.*, vol. 36, pp. 165-171, 1989.

[4] M. X. Huang, J. C. Mosher, and R. M. Leahy, "A sensor-weighted overlapping-sphere head model and exhaustive head model comparison for MEG," *Physics In Medicine And Biology*, vol. 44, pp. 423-440, 1999.

[5] J. Li, H. Y. Zhu, and S. L. He, "Fast method for the localisation of current dipoles in the human brain," *Medical & Biological Engineering & Computing*, vol. 39, pp. 678-680, 2001.

[6] J. Rahola and S. Tissari, "Iterative solution of dense linear systems arising from the electrostatic integral equation in MEG," *Physics In Medicine And Biology*, vol. 47, pp. 961-975, 2002.

[7] A. Tarkiainen, M. Liljestrom, M. Seppa, and R. Salmelin, "The 3D topography of MEG source localization accuracy: effects of conductor model and noise," *Clinical Neurophysiology*, vol. 114, pp. 1977-1992, 2003.

[8] J. Sarvas, "Basic mathematical and electromagnetic concepts of the biomagnetic inverse problem," *Phys. Med. Biol.*, vol. 32, pp. 11-22, 1987.

[9] H. M. Uutela K, Salmelin R, "Global optimization in the localization of neuromagnetic sources," *IEEE. Trans. Biomed. Eng.*, vol. 45, pp. 716—723, 1998.

[10] J. C. Mosher and R. M. Leahy, "Source localization using recursively applied and projected (RAP) MUSIC," *Ieee Transactions On Signal Processing*, vol. 47, pp. 332-340, 1999.

[11] J. C. Mosher, R. M. Leahy, and P. S. Lewis, "EEG and MEG: Forward solutions for inverse methods," *IEEE Transactions On Biomedical Engineering*, vol. 46, pp. 245-259, 1999.

[12] B. Yvert, A. Crouzeix-Cheylus, and J. Pernier, "Fast realistic modeling in bioelectromagnetism using lead-field interpolation," *Human Brain Mapping*, vol. 14, pp. 48-63, 2001.